NRC Research Press

The cation–anion interaction in ionic liquids studied by extractive electrospray ionization mass spectrometry

Yafei Zhou, Junfeng Zhan, Xiang Gao, Cao Li, Konstantin Chingin, and Zhanggao Le

Abstract: Ionic liquids, known as green solvents, are of sustainable interest in modern chemistry, industry, and many other fields. Here, extractive electrospray ionization has been applied to transfer various room temperature ionic liquids into the gas phase for mass spectrometry analysis. Generated mass spectra display free cations (C^+), anions (A^-), and small salt clusters, such as C_2A^+ and CA_2^-, from strongly diluted ionic liquid samples ($<10^{-8}$ mol/L) with high sensitivity and tolerance to chemical contamination. The eight ionic liquids based on the 1-butyl-3-methylimidazolium cation with different anions (OH^-, HSO_4^-, Cl^-, BF_4^-, $AlCl_4^-$, NO_3^-, Ac^-, and PF_6^-) are investigated in the present work. Interestingly, the 1-butyl-3-methylimidazolium cation signal intensity is inversely correlated with the hydrogen bonding strength between the anion and cation. Our study indicates that the direct extractive electrospray ionization mass spectrometry analysis is a convenient method to screen ionic liquid libraries with regard to chemical composition, physicochemical properties, and supramolecular organization of ionic liquids.

Key words: extractive electrospray ionization tandem mass spectrometry, room temperature ionic liquids, interactions, hydrogen bonding, chemical contamination, viscous samples.

Résumé : Les liquides ioniques, connus sous le nom de solvants verts, présentent un intérêt écologique dans la chimie et l'industrie modernes et dans de nombreux autres domaines. Ici, l'ionisation par électronébulisation extractive a été utilisée pour transférer des liquides ioniques, à différents liquides ioniques à température ambiante vers la phase gazeuse afin d'effectuer une analyse par spectrométrie de masse. Les spectres de masse obtenus mettent en évidence la présence de cations (C^+) et d'anions (A^-) libres et de petites agrégats de sel, notamment sous forme d'ions C_2A^+ et CA_2^-, formés à partir d'échantillons fortement dilués de liquide ionique (de concentration inférieure à 10^{-8} mol/L) ayant une sensibilité et une tolérance élevées à la contamination chimique. Les huit liquides ioniques formés à partir du cation 1-butyl-3-méthylimidazolium (Bmim) et de différents anions (OH^-, HSO_4^-, Cl^-, BF_4^-, $AlCl_4^-$, NO_3^-, Ac^- et PF_6^-) sont ici étudiés. De façon intéressante, on constate que l'intensité du signal correspondant au 1-butyl-3-méthylimidazolium est inversement proportionnel à la force de a liaison hydrogène entre l'anion et le cation. Notre étude indique que l'analyse directe par spectrométrie de masse et l'ionisation par électronébulisation extractive est une méthode pratique pour inventorier les liquides ioniques selon leur composition chimique, leurs propriétés physico-chimiques et leur organisation supramoléculaire. [Traduit par la Rédaction]

Mots-clés : Ionisation par électronébulisation extractive couplée à la spectrométrie de masse, liquides ioniques à température ambiante, interactions, liaison hydrogène, contamination chimique, échantillons visqueux.

Introduction

Room temperature ionic liquids (RTILs) are a class of organic salts with several unique properties such as liquidity at room temperature, high thermal stability, and low volatility. ILs are widely applied in organic synthesis, catalysis, and electrochemistry as a novel class of environmentally friendly solvents or reaction media.[1–3] ILs are known as "designer solvents" because their properties including melting point, viscosity, density, and hydrophobicity can be tailored by the appropriate selection of ions.[4] The properties of ILs and IL-mediated reactions can often be predicted and tuned based on the intrinsic strength of the cation–anion interaction. Thus, strong cation–anion bonding is known to reduce the interaction between the cation and transition-state species as well as to reduce the interaction between the anion and electrophilic species.[5,6]

The energy of the cation–anion interaction and the structure of ILs have been probed by several approaches, such as X-ray diffraction,[7,8] midinfrared,[9] far-infrared,[10] attenuated total reflection infrared,[11] Raman scattering,[12] and NMR spectroscopy,[13,14] as well as using ab initio and density functional theory (DFT) calcula-

tions.[10,15,16] Mass spectrometry was first applied to explore the properties of diluted ILs more than two decades ago.[17] Recently, electrospray ionization mass spectrometry (ESI-MS) was used to visualize the composition of IL aggregates in solution and probe the relative interaction energies combined with the theoretical calculation.[18–20]

In present work, the cation–anion interaction in highly diluted solutions was explored by extractive electrospray ionization mass spectrometry (EESI-MS). EESI is a much softer variation of ESI ionization,[21–23] allowing the preservation of weakly bound species upon their transfer from the solution into the gas phase. Our results for eight different 1-butyl-3-methylimidazolium (Bmim) ILs suggests that the intensity of free cations in EESI mass spectra can be used as a direct measure to quantify the energy of the cation–anion interaction.

Experimental section

Reagents

The RTILs (impurities ≤ 1%), as shown in Table 1 and their chemical structures in Chart 1, were purchased from Shanghai
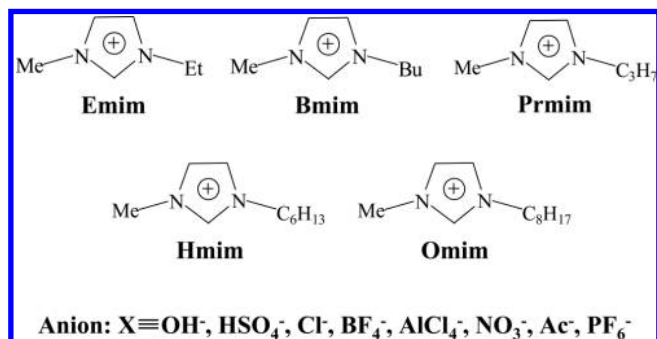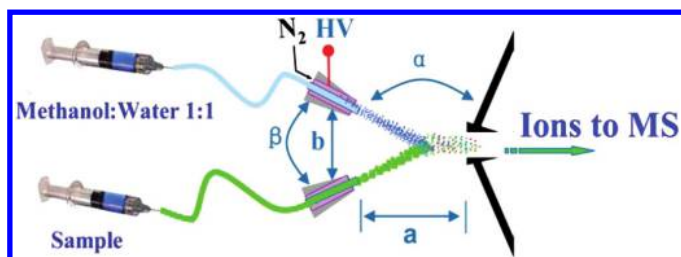
Y. Zhou, J. Zhan, X. Gao, C. Li, K. Chingin, and Z. Le. East China Institute of Technology, 418 Guanglan Road, Nanchang City, Jiangxi Province 330013, P.R. China.
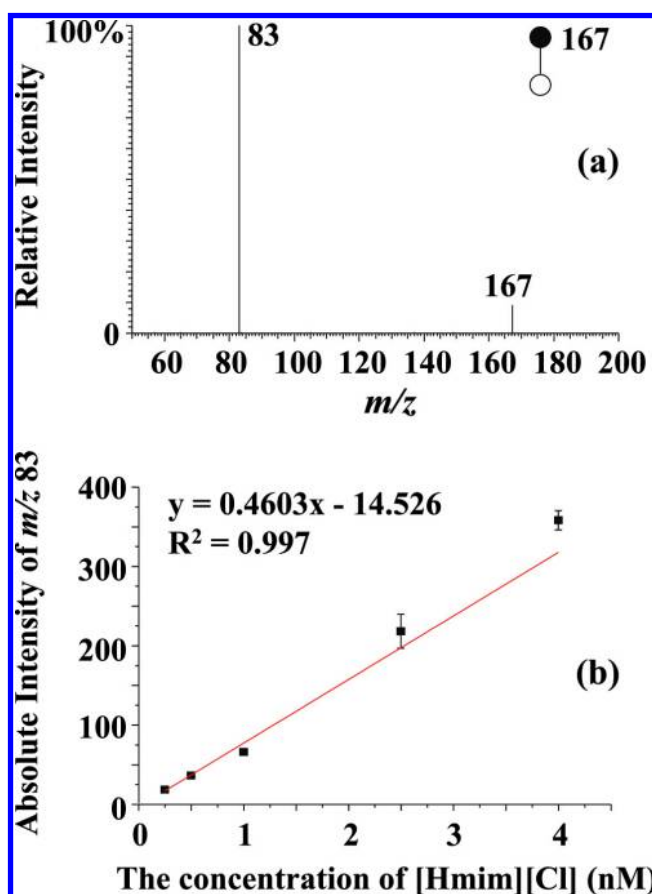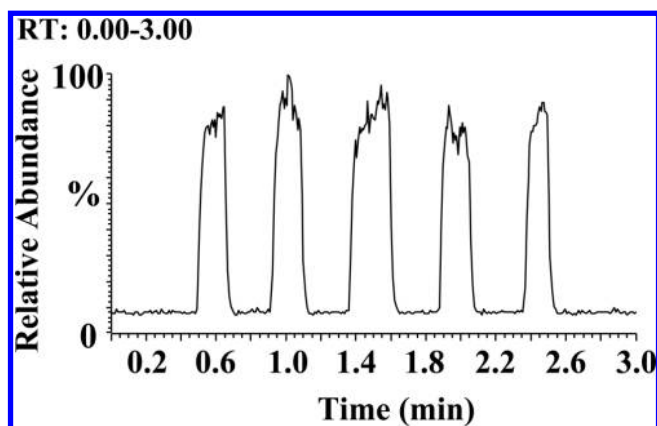
Corresponding author: Zhanggao Le (e-mail: zhgle@ecit.cn).

Table 1. Essential information for the ILs.

Number	Compound	Abbreviation	Molecular weight
1	1-Ethyl-3-methylimidazolium hydroxide	[Emim][OH]	128
2	1-Propyl-3-methylimidazole hydroxide	[Prmim][OH]	142
3	1-Butyl-3-methylimidazolium hydroxide	[Bmim][OH]	156
4	1-Octyl-3-methylimidazole hydroxide	[Omim][OH]	212
5	1-Butyl-3-methylimidazole six fluoride phosphate	[Bmim][PF$_6$]	284
6	1-Octyl-3-methylimidazole six fluoride phosphate	[Omim][PF$_6$]	340
7	1-Hexyl-3-methylimidazole chloride	[Hmim][Cl]	203
8	1-Butyl-3-methylimidazole chloride	[Bmim][Cl]	175
9	1-Ethyl-3-methylimidazole four fluoroborate	[Emim][BF$_4$]	198
10	1-Propyl-3-methylimidazole iodide	[Prmim][I]	252
11	1-Butyl-3-methylimidazolium hydrogen sulfate	[Bmim][HSO$_4$]	236
12	1-Butyl-3-methylimidazolium acetate	[Bmim][Ac]	198
13	1-Butyl-3-methylimidazolium nitrate	[Bmim][NO$_3$]	201

Chart 1.

Anion: X≡OH⁻, HSO$_4^-$, Cl⁻, BF$_4^-$, AlCl$_4^-$, NO$_3^-$, Ac⁻, PF$_6^-$

Fig. 1. Schematic diagram for the direct analysis of ionic liquids by EESI-MS. Note that the diagram is not proportionally scaled.
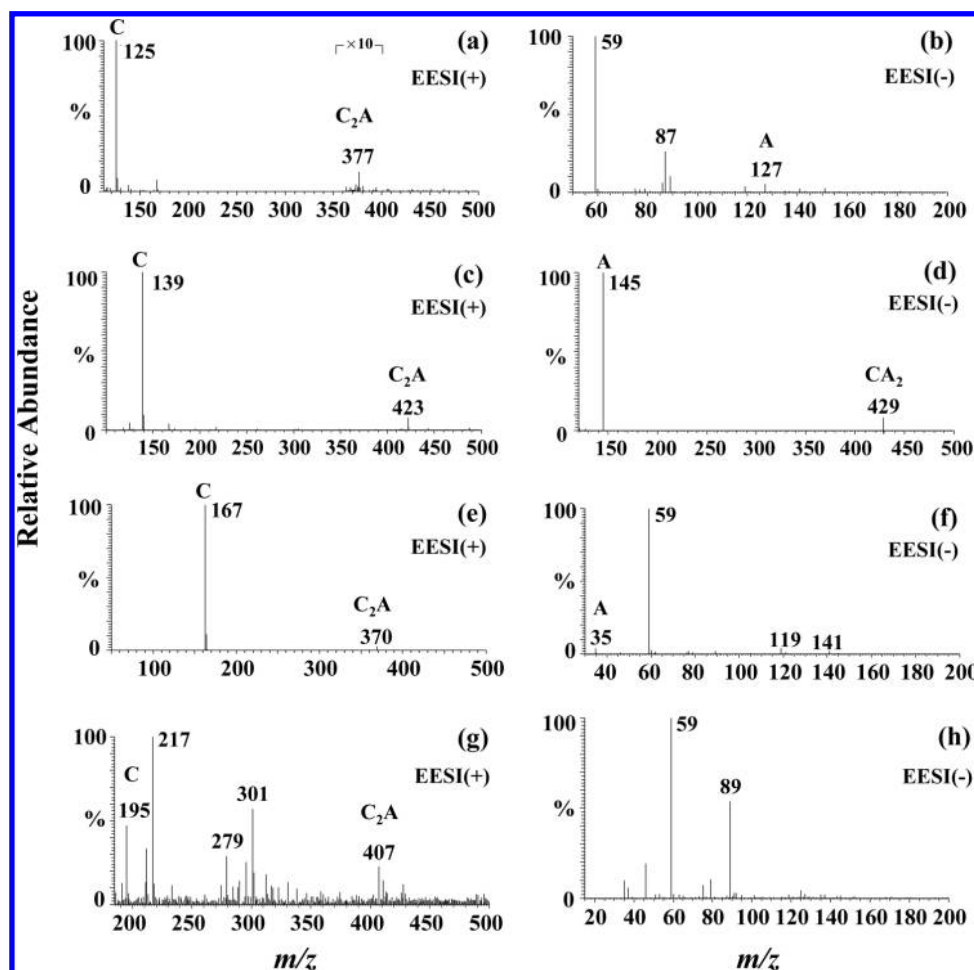

Cheng Jie Chemical Co. Ltd. (Shanghai, China). HPLC-grade methanol was purchased from ROE Scientific, Inc. (Newark, New Jersey). Water was purified and deionized in house to Milli-Q grade. All of the ILs were diluted to a concentration of 1 ppb in methanol, which roughly corresponds to 10^{-9} mol/L for MS analysis.

Fig. 2. Quantitative analysis of IL [Hmim][Cl] detected by EESI-MS from methanol solutions. (*a*) MS/MS analysis of cation Hmim (*m/z* 167); the neutral loss of the 84 u fragment (C$_6$H$_{12}$) was observed at *m/z* 83. (*b*) The calibration curve obtained by EESI-MS shows a good linearity within the concentration range of 0.25–4.0 nmol/L (R^2 = 0.997).

Fig. 3. Single-ion chromatogram of the *m/z* 167 cationic signal during EESI-MS analysis of diluted [Hmim][Cl] in methanol (10^{-9} mol/L). Five successive and stable samplings feature high throughput and reproducibility.

Experimental setup

All experiments were carried out using a commercial linear ion trap mass spectrometer (LTQ-XL) (Finnigan, San Jose, California) coupled with a homemade EESI source. The primary part of experimental setup is schematically shown in Fig. 1 as previously reported.[24,25] Herein, the angle *α* between the spray

Fig. 4. EESI mass spectra of [Prmim][I], [Bmim][PF$_6$], [Hmim][Cl], and [Omim][OH] diluted in methanol (10^{-9} mol/L) obtained in positive mode (left panels) and negative mode (right panels).

outlet and the heated capillary of the LTQ instrument was maintained at about 150°, which was equivalent to the angle between sample beam and the heated capillary of the LTQ instrument. The angle β between the sample plume outlet and the electrospray beam was about 60°. The distance a between the inlet of the LTQ instrument and the electrospray gas outlet was 10 mm. The distance b between the two spray tips was 1.5 mm.

The pure methanol–water mixture (1:1, v/v) and IL sample were introduced via identical fused silica capillaries (i.d. = 0.1 mm, o.d. = 0.19 mm) using a conventional pumping system (PHD ULTRA^{TM} CP) (Harvard Apparatus, Holliston, Massachusetts) at the same flow rate of 5 μL/min. The heated capillary temperature was optimized to 150 °C. Ionizing voltage was applied to the syringe (Thermo, USA) and set as ±3.5 kV in positive and negative ion detection mode, respectively. The mass scan ranges were from m/z 50 to 1000 and from 15 to 200. Nebulizing nitrogen gas for both sprayers was supplied at a pressure of 1.0 MPa via stainless steel capillaries (i.d. = 0.25 mm, o.d. = 1.59 mm). Other parameters were used without further optimization. Collision-induced dissociation experiments were performed by applying normalized collision energies 15%–32% to the precursor ions isolated with a mass-to-charge window width of 1.4 u and 30 ms activation time.

Results and discussion

EESI-MS of ILs

ILs, a class of organic salts, exhibit interesting physicochemical properties that depend on the nature of cation and anion.

MS has been applied to investigate ILs with high sensitivity and selectivity. The limit of detection of EESI-MS is generally low for the analysis of many compounds.[21,26–28] In this study, the limit of detection of EESI-MS/MS measurements following 1-hexyl-3-methylimidazole chloride ([Hmim][Cl]) fragment m/z 83 generated from Hmim cation (m/z 167) is estimated to be 16 pmol/L and a relative standard deviation (RSD) of 4.0%–12.1% ($S/N \geq 3$, $n = 5$). Figure 2 shows the quantitative analysis of IL [Hmim][Cl] detected by EESI-MS from methanol solutions. Figure 2a shows MS/MS analysis of the cation (Hmim, m/z 167); the neutral loss of the 84 u fragment (C_6H_{12}) is observed m/z 83;. Figure 2b shows the calibration curve based on the dependence of the concentration of [Hmim][Cl] versus the intensity of the fragment ion m/z 83 obtained by EESI-MS, showing a good linearity within the concentration range of 0.25~4.0 nmol/L (R^2 = 0.997). Furthermore, Fig. 3 shows a single-ion chromatogram of the m/z 167 cationic signal during EESI-MS analysis of diluted [Hmim][Cl] in methanol (10^{-9} mol/L). Five successive and stable samplings are shown, featuring high throughput and reproducibility. The results suggest that EESI-MS is an ideal tool for analysis of ILs.

Figure 4 shows EESI mass spectra of four different ILs, [Prmim][I], [Bmim][PF$_6$], [Hmim][Cl], and [Omim][OH], diluted in pure methanol to a concentration of 10^{-9} mol/L. In EESI(+), the characteristic signals were detected corresponding to IL cations Prmim$^+$ at m/z 125, Bmim$^+$ at m/z 139, Hmim$^+$ at m/z 167, and Omim$^+$ at m/z 195 at high intensity as well as weak C$_2$A$^+$ cluster

signals (Fig. 4, left panels). Peak assignments are supported by the MS/MS analysis of corresponding signals (Fig. 5). In MS/MS, all C+ signals produce 1-methyl-imidazole positive ions and C_2A^+ clusters produce C+ signals. In EESI(–), we only observe free anion (PF_6^- at m/z 145) and CA_2^- (m/z 429) for [Bmim][PF_6]. However, CA_2^- cluster signals are not detected in the other three ILs (Fig. 4, right panels). Interestingly, for the IL [Omim][OH], even the free anion OH$^-$ at m/z 17 cannot be observed in EESI(–) (Fig. 4h).

Cation−anion interaction in ILs

By now, considerable evidence has been accumulated by other work that the ESI mass spectra of diluted ILs reflect their composition in neat (nondiluted) state. For example, the "magic"-numbered cluster peaks ($C^{n+1}A^n$) of imidazolium ILs in ESI-MS were found to be in agreement with the high stability of these clusters as predicted by theoretical calculations.[20] The good correlation between ESI-MS signal intensity for diluted samples and the binding strength of nondiluted samples can be due to the low volatility of ILs. Thus, IL components are evaporated from ESI droplets at a much lower rate compared with water and organic solvents. As a result, IL becomes much more concentrated in mature droplets and its behaviour more resembles that of neat IL.
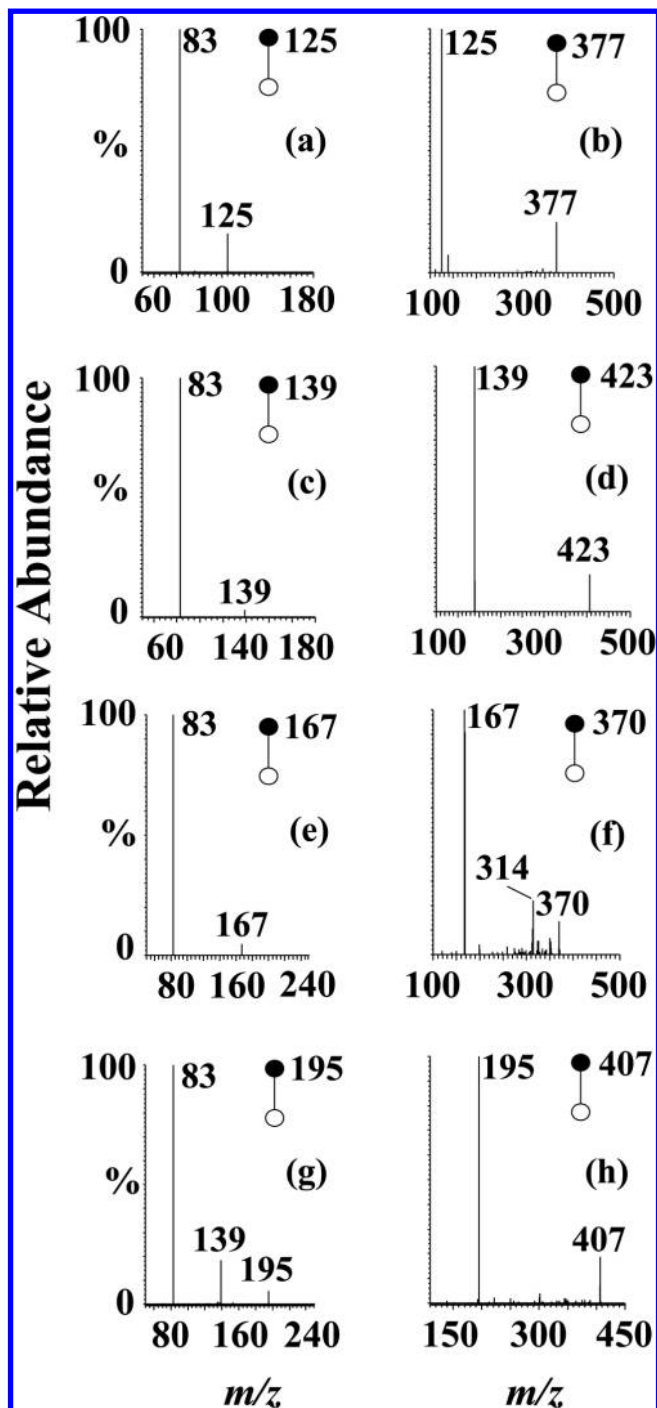
Our data suggest that the strength of cation–anion bonding in ILs can be directly estimated from their EESI mass spectra (as shown in Fig. 6). We compare the EESI(+) mass spectra of eight diluted Bmim ILs (10^{-9} mol/L in methanol) with different anions (OH$^-$, HSO$_4^-$, Cl$^-$, BF$_4^-$, AlCl$_4^-$, NO$_3^-$, Ac$^-$, and PF$_6^-$) by EESI-MS (Fig. 6a). The signal intensity of the free Bmim cation is the highest with the OH$^-$ anion and decreases for the other ILs in the following order: [OH]$^-$ ≈ [AlCl$_4$]$^-$ > [HSO$_4$]$^-$ > [Cl]$^-$ > [BF$_4$]$^-$ > [NO$_3$]$^-$ > [PF$_6$]$^-$ ≈ [Ac]$^-$. Moreover, Fig. 6b shows the correlation of the experimental data obtained by EESI-MS and the reported DFT data[11] based on the investigated five Bmim ILs (10^{-9} mol/L in methanol) with different anions such as OH$^-$, HSO$_4^-$, Cl$^-$, BF$_4^-$, and PF$_6^-$. Unfortunately, we are able to find reference literature data reported for only five Bmim ILs (OH$^-$, HSO$_4^-$, Cl$^-$, BF$_4^-$, and PF$_6^-$) out of the eight studied in this work. Hence the difference in the number of data points in Figs. 6a and 6b. Interestingly, the observed dependence is in very good agreement with the energies of hydrogen bonding reported by vibrational spectroscopy.[11]

By comparing the present experimental data and reported calculated values[11] for these eight ILs based on the Bmim cation with different anions, it was found that the cohesive energies (ΔE) calculated by DFT are not completely coherent with the present experimental orders. The ΔE values for BmimCl are larger than those for BmimHSO$_4$, BmimBF$_4$, and BmimPF$_6$. A probable explanation for this abnormal energy value is that the size of the chlorine ion is much smaller than the other three anions, and the chlorine ions are closer to the imidazolium cation so that the cation–anion interactions of $^+C–H\cdots Cl^-$ are probably stronger than for the other ILs. Overall, the stronger the hydrogen binding, the weaker is the intensity of the free Bmim signal. We conclude that the signal intensity for the free cation reflects the dissociation constant of IL in solution and can be used to directly quantify the energy of the cation–anion interaction.
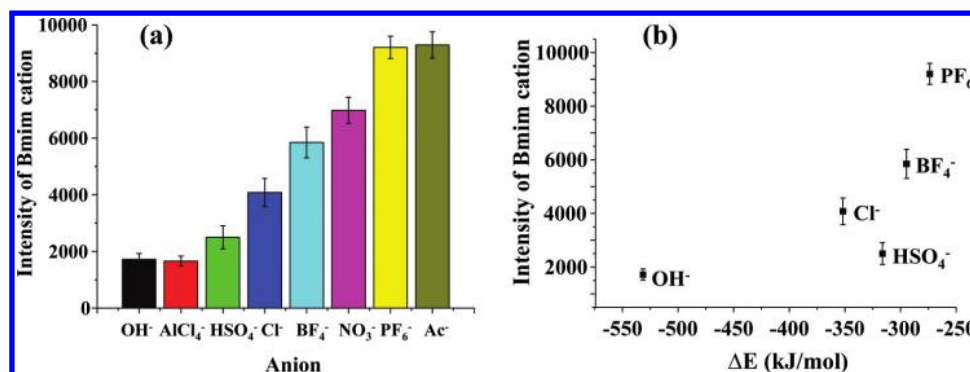
Conclusion

We probed the IL aggregates in methanol solution and hydrogen bonding between cation and anion in ILs with low concentrated solutions (10^{-9} mol/L) by EESI-MS. On the basis that the limit of detection of ILs investigated roughly is 16 pmol/L, we can observe free cations (C+), anions (A$^-$), and small salt clusters such as C_2A^+ and CA_2^- from strongly diluted IL samples (<10^{-8} mol/L) by using tandem MS. Moreover, the relative

Fig. 5. EESI-MS/MS spectra of cations (left panels) and C_2A clusters (right panels) detected from [Prmim][I], [Bmim][PF_6], [Hmim][Cl], and [Omim][OH] diluted in methanol (10^{-9} mol/L) in positive detection mode.

hydrogen bonding strength of eight Bmim-based ILs between cation and anion are investigated, and the sequence is [OH]$^-$ ≈ [AlCl$_4$]$^-$ > [HSO$_4$]$^-$ > [Cl]$^-$ > [BF$_4$]$^-$ > [NO$_3$]$^-$ > [PF$_6$]$^-$ ≈ [Ac]$^-$, which is in good agreement with that reported, suggesting that direct EESI-MS is a useful tool to reflect the interaction energy between cations and anions in ILs with high sensitivity, throughput, reproducibility, and tolerance to chemical contamination.

Fig. 6. EESI(+)-MS analysis of eight diluted Bmim ILs (10^{-9} mol/L in methanol) with different anions: (*a*) comparison of the intensity of the Bmim cation; (*b*) correlation of the experimental data obtained by EESI-MS and the reported DFT data based on the investigated five Bmim ILs. The Bmim signal intensity is inversely correlated with the strength of hydrogen bonding between the cation and anion.

Acknowledgements

References

(1) Chiappe, C.; Pieraccini, D. *J. Phys. Org. Chem.* **2004**, *18* (4), 275. doi:10.1002/poc.863.
(2) Sun, P.; Armstrong, D. W. *Anal. Chim. Acta* **2010**, *661* (1), 1. doi:10.1016/j.aca.2009.12.007.
(3) Han, X.; Armstrong, D. W. *Acc. Chem. Res.* **2007**, *40* (11), 1079. doi:10.1021/ar700044y.
(4) Earle, M. J.; Seddon, K. R. *Pure Appl. Chem.* **2000**, *72* (7), 1391. doi:10.1351/pac200072071391.
(5) Aggarwal, A.; Lancaster, N. L.; Sethi, A. R.; Welton, T. *Green Chem.* **2002**, *4* (5), 517. doi:10.1039/b206472c.
(6) Chiappe, C.; Pieraccini, D. *Green Chem.* **2003**, *5* (2), 193. doi:10.1039/b211340f.
(7) Roth, C.; Peppel, T.; Fumino, K.; Köckerling, M.; Ludwig, R. *Angew. Chem. Int. Ed.* **2010**, *49* (52), 10221. doi:10.1002/anie.201004955.
(8) Song, X.; Hamano, H.; Minofar, B.; Kanzaki, R.; Fujii, K.; Kameda, Y.; Kohara, S.; Watanabe, M.; Ishiguro, S.-i.; Umebayashi, Y. *J. Phys. Chem. B* **2012**, *116* (9), 2801. doi:10.1021/jp209561t.
(9) Viell, J.; Marquardt, W. *Appl. Spectrosc.* **2012**, *66* (2), 208. doi:10.1366/11-06427.
(10) Fumino, K.; Wulf, A.; Ludwig, R. *Angew. Chem. Int. Ed.* **2008**, *47* (20), 3830. doi:10.1002/anie.200705736.
(11) Gao, Y.; Zhang, L.; Wang, Y.; Li, H. *J. Phys. Chem. B* **2010**, *114* (8), 2828. doi:10.1021/jp910528m.
(12) Roth, C.; Chatzipapadopoulos, S.; Kerlé, D.; Friedriszik, F.; Lütgens, M.; Lochbrunner, S.; Kühn, O.; Ludwig, R. *New J. Phys.* **2012**, *14* (10), 105026. doi:10.1088/1367-2630/14/10/105026.
(13) Cremer, T.; Kolbeck, C.; Lovelock, K. R.; Paape, N.; Wölfel, R.; Schulz, P. S.; Wasserscheid, P.; Weber, H.; Thar, J.; Kirchner, B. *Chem-Eur. J.* **2010**, *16* (30), 9018. doi:10.1002/chem.201001032.
(14) Wulf, A.; Fumino, K.; Ludwig, R. *Angew. Chem. Int. Ed.* **2010**, *49* (2), 449. doi:10.1002/anie.200905437.
(15) Dong, K.; Zhang, S.; Wang, D.; Yao, X. *J. Phys. Chem. A* **2006**, *110* (31), 9775. doi:10.1021/jp054054c.
(16) Wang, Y.; Li, H.; Han, S. *J. Chem. Phys.* **2005**, *123*, 174501. doi:10.1063/1.1979478.
(17) Ackermann, B. L.; Tsarbopoulos, A.; Allison, J. *Anal. Chem.* **1985**, *57* (8), 1766. doi:10.1021/ac00285a060.
(18) Fernandes, A. M.; Rocha, M. A.; Freire, M. G.; Marrucho, I. M.; Coutinho, J. A.; Santos, L. M. *J. Phys. Chem. B* **2011**, *115* (14), 4033. doi:10.1021/jp201084x.
(19) Bini, R.; Bortolini, O.; Chiappe, C.; Pieraccini, D.; Siciliano, T. *J. Phys. Chem. B* **2007**, *111* (3), 598. doi:10.1021/jp0663199.
(20) Gozzo, F. C.; Santos, L. S.; Augusti, R.; Consorti, C. S.; Dupont, J.; Eberlin, M. N. *Chem-Eur. J.* **2004**, *10* (23), 6187. doi:10.1002/chem.200305742.
(21) Gu, H. W.; Xu, N.; Chen, H. W. *Anal. Bioanal. Chem.* **2012**, *403* (8), 2145. doi:10.1007/s00216-012-5874-1.
(22) Chen, H. W.; Yang, S. P.; Li, M.; Hu, B.; Li, J. Q.; Wang, J. *Angew. Chem.* **2010**, *122* (17), 3117. doi:10.1002/ange.200906886.
(23) Ma, X.; Zhang, S.; Zhang, X. *Trends Anal. Chem.* **2012**, *35*, 50. doi:10.1016/j.trac.2011.12.004.
(24) Law, W. S.; Wang, R.; Hu, B.; Berchtold, C.; Meier, L.; Chen, H.; Zenobi, R. *Anal. Chem.* **2010**, *82* (11), 4494. doi:10.1021/ac100390t.
(25) Liu, C.; Zhang, X.; Xiao, S.; Jia, B.; Cui, S.; Shi, J.; Xu, N.; Xie, X.; Gu, H.; Chen, H. *Talanta* **2012**, *98*, 79. doi:10.1016/j.talanta.2012.06.048.
(26) Chen, H. W.; Hu, B.; Hu, Y.; Huan, Y. F.; Zhou, Z. Q.; Qiao, X. L. *J. Am. Soc. Mass. Spectrom.* **2009**, *20* (4), 719. doi:10.1016/j.jasms.2008.12.011.
(27) Zhu, L.; Gamez, G.; Chen, H. W.; Chingin, K.; Zenobi, R. *Chem. Commun.* **2009**, (5), 559. doi:10.1039/B818541G.
(28) Wu, Z. C.; Zhou, Y. F.; Xu, N.; Tao, L.; Chen, H. W. *J. Anal. At. Spectrom.* **2013**, *28* (5), 697. doi:10.1039/c3ja00011g.